Performance and Emissions of a Premixed Combustion Engine Fueled by Methanol–Gasoline Blends

Jibai Wang (2012022005@chd.edu.cn)
Chang'an University
Peng Zhang
Chang'an University
Chunhua Zhang
Chang'an University
Zheng Jing
Chang'an University

Original article

Keywords: Internal combustion engine, Methanol–gasoline blend, Unregulated emission, Compression ratio

Posted Date: June 2nd, 2020

DOI: https://doi.org/10.21203/rs.3.rs-32148/v1

Abstract

Background: Methanol is abundant, safe, and environmentally friendly and has physicochemical properties similar to those of gasoline. It is a promising alternative fuel in China because it can be directly used in both spark- and compression-ignition internal combustion engines. The current development of spark-ignition engines focuses on the reduction of the fuel volume and increase in the compression ratio (CR), which would benefit the engine's thermal efficiency. However, increasing the CR may deteriorate particulate matter (PM) due to the high temperature.

Methods: Herein, an experimental study was conducted on methanol–gasoline blends in a spark-ignition engine. We examined the performance and formaldehyde emissions of methanol–gasoline blends by using three volume fractions (M0, M15, and M100). In addition, the effects of the CR on PM emissions were investigated.

Results: The following relationships were observed: (1) When methanol was blended with gasoline, the formaldehyde emissions increased significantly. The formaldehyde emissions of 100% methanol were higher than those of the methanol–gasoline blend with a methanol volume fraction of 15%; both of these emissions were higher than those of pure gasoline; (2) Increasing the CR resulted in increased PM emissions; (3) For a given blending ratio, the PM emissions were positively correlated with the CR; and (4) The PM emissions were negatively correlated with the methanol volume fraction.

Conclusions: Methanol reduces the heat loss at the wall surface. As the ratio of methanol in gasoline increases, the PM emissions decrease. On the other hand, the PM emissions are positively correlated with the CR. The addition of lower alcohols dilutes the concentrations of soot precursors, thereby reducing the soot emissions.

Background

The internal combustion engine continues to play a vital role in the field of transportation because of its advantages such as an excellent reliability, wide applicability, and high work efficiency (Huang et al., 2017). Because of the imbalance of the supply and demand for petroleum resources and increasingly strict emission regulations, the development of biofuels as replacements of traditional fuels, such as gasoline and diesel, and solutions to mitigate pollution arising from traditional fuel emissions have become key areas of research worldwide. Prior investigations have relied on the following approaches to reduce emission-related pollution and to further improve the thermal efficiency of internal combustion engines. First, fuel-reforming methods (Tartakovsky and Sheintuch, 2018) can be used to crack hydrogen and free radicals by using waste heat in the form of exhaust gas. The hydrogen in these cracked products enhances the flame velocity, thus improving the fuel efficiency and reducing emissions. Second, the use of oxygen-containing fuels as additives can significantly reduce soot emissions when the oxygen content of the fuel mixture exceeds 30% (Liu et al., 2017). In addition, emissions of nitrogen oxides and greenhouse gases (GHGs), such as carbon dioxide, can be reduced by using fuels based on alcohols

because of the large latent heat of vaporization associated with alcohols as well as the low carbon contents relative to gasoline and diesel (Tucki et al., 2019). Third, in addition to the above-mentioned two methods, a dual-fuel approach can also be employed. Both spark- and compression-ignition engines can use dual fuels to increase the thermal efficiency and reduce emissions (Cheng et al., 2008; Hagos et al., 2017; Huang et al., 2017; Bharathiraja et al., 2019). Fourth, novel in-cylinder combustion modes can be established, such as exhaust gas recirculation (EGR), optimized injection strategies, and improved in-cylinder turbulence or vortex intensities. Fifth, emissions can be reduced by using a combination of post-combustion treatments, including selective catalytic reduction (SCR), diesel particle filtering (DPF), diesel oxidation catalysts (DOC), gasoline particulate filtering (GPF), three-way catalysts (TWC), and lean NO_x trapping (LNT; Frenklach, 2002; Reitz and Duraisamy, 2015; Kumar and Saravanan, 2016; Benajes et al., 2017; Yue and Reitz, 2019).

Among these measures, the use of oxygen-containing fuel additives has the following advantages: technological feasibility, low cost, and pronounced emissions reduction effects. Because of the advantages introduced by the regeneration of conventional fuels, considerable efforts have been made to save carbon and improve emission profiles; consequently, lower alcohols, that is, mainly methanol and ethanol, have recently received significant attention.

In China and globally, methanol and ethanol are widely commercially used as vehicle fuels. Methanol and ethanol are linearly structured lower alcohols that yield low carbon emissions. Tucki et al. (2019) studied the carbon dioxide emissions of biofuels by using the New European Driving Cycle (NEDC). Their results suggested that adding biofuels to gasoline can significantly reduce carbon dioxide emissions, but, at the same time, can lead to the increase in the consumption of biofuels. Ethanol is highly miscible with water, which causes an inevitable problem when ethanol is used as a vehicle fuel; under both dry and wet conditions, ethanol can cause the severe corrosion of metallic circuits and nonmetallic rubber materials (Jin et al., 2011). On the other hand, coal reserves account for a large proportion of the energy structure in China, whereas methanol can be obtained by employing multiple techniques (Awad et al., 2018). The four standard processes used to synthesize methanol are coal-to-methanol synthesis, coke oven gas reform, carbon dioxide-to-methanol synthesis (Samimi et al., 2018), and natural gas-to-methanol synthesis. The cost of synthesizing methanol from coal is lower than the costs of synthesizing methanol from natural gas and coke oven gas. The global methanol production capacity has increased since 2011 and the production capacity reached 84.317 million tons in 2018, which represents an annual increase of 1%. Methanol can be used to produce hydrocarbons (Chen et al., 2019), olefins, and gasoline. Yarulina et al. (2018) investigated the effects of the topology and acidity of zeolitic catalysts on the synthesis of olefins from methanol. Specifically, Yarulina et al. (2018) examined the promotional effects of silica and alumina–zeolite catalysts on the alkene cycle. Sharifi et al. (2019) analyzed the effects of the ratio of silica to alumina on the hydrodesulfurization process and the catalytic conversion efficiency of methanol. Huang et al. (2018) investigated the effects of acidic substances in methanol on the efficiency of the methanol-to-gasoline conversion. The low cost of coal-to-methanol synthesis and the widespread

applications of methanol suggest that the development of coal-to-methanol synthesis is more appropriate regarding China's energy consumption.

Researchers are currently drawn toward renewable resources and methanol extracted via black liquor co-gasification has become a popular choice (Carvalho et al. 2018).

As a simple alcohol-based fuel, methanol is a colorless, transparent, and volatile water-soluble liquid with a slight alcoholic taste. Table 1 lists the physicochemical properties of methanol.

Table 1
Comparison of physicochemical properties of methanol and gasoline

Property	Gasoline	Methanol
Chemical formula	C_4–C_{12} hydrocarbon compounds	CH_3OH
Relative molecular mass	95–120	32
Carbon content (%)	85–88	37.5
Oxygen content (%)	0–0.1	50
Density (25 °C)/(kg/L)	0.70–0.78	0.795–0.801
Boiling point (°C)	30–200	64.8
Latent heat of vaporization (kJ/kg)	310	1109
Saturated vapor pressure (bar)	62.0–82.7	30.997
Theoretical air-fuel ratio	14.73	6.36
Lower heating value (MJ/kg)	43.5	19.7

The low heating value (LHV), high octane number, and low cetane number render methanol suitable for the application as fuel. Wang et al. (2019) experimentally investigated the cooling effect of methanol and determined that the reduction of the LHV of methanol blends leads to a poor break specific fuel consumption (BSFC), which is partially offset by the thermal efficiency. Yao et al. (2008) modified the fuel supply and combustion modes on a diesel engine to increase the power of the internal combustion engine, reduce emissions, and demonstrate the dual-fuel mode operation of methanol and diesel. Wang et al. (2015) developed an electronic control unit (ECU) based on the diesel/methanol compound combustion (DMCC) mode in which the dual-fuel operation of diesel and methanol was realized to examine the fuel economy of a diesel/methanol dual-fuel engine. Their results indicated that a diesel/methanol mixture can reduce the fuel consumption of an engine compared with pure diesel. This dual-fuel mode, however, requires the addition of a new fuel supply system. Methanol has a higher octane number than gasoline, which implies that methanol is more suitable for spark-ignition engines and does not require the change of the structural parameters of the internal combustion engine. Furthermore, the blended combustion of methanol and gasoline has been thoroughly investigated in previous studies.

When methanol and gasoline are mixed with a volume fraction above 25% but below 75%, phase separation occurs. Therefore, the addition of a co-solvent is required when using a blended fuel of methanol and gasoline. Schifter et al. (2019) and Rosdia et al. (2019) independently conducted experimental studies on the effects of co-solvents on the physicochemical properties of methanol–gasoline blends as well as their power and fuel economy. The addition of isopropyl alcohol as a co-solvent reduced the Reid vapor pressure of the methanol–gasoline blends, whereas an increase in the 1,2-propylene glycol content as a co-solvent reduced the power of the methanol–gasoline engine. Nonetheless, the torque of the engine increased slightly; when the added amount was 8 mL/L, the power only slightly decreased without affecting the torque. Shirazi et al. (2019) studied the effect of the blending ratio of lower and higher alcohols on the physicochemical characteristics such as the saturated vapor pressure and kinematic viscosity. Their results showed that by using fuel blends of lower alcohols, such as methanol, and higher alcohols, such as n-butanol and pentanol, problems associated with the highly saturated vapor pressure and low kinematic viscosity of alcohol fuels can be simultaneously solved. Tian et al. (2018) conducted an experimental study of pool fires in a full-scale tunnel regarding the storage and transportation safety of methanol–gasoline blends.

However, there is a lack of studies of the effects of unregulated emissions when methanol–gasoline blends are used as fuel. Numerous studies have been performed to identify a suitable alternative fuel that decreases exhaust emissions and enhances the power output. Dabas et al. (2019) conducted experimental studies on the power, fuel economy, and emissions of internal combustion engines using methanol–gasoline and ethanol–gasoline blends. The results for internal combustion engines using methanol–gasoline blends indicated that the nitrogen oxide emissions increased, the carbon monoxide and hydrocarbon emissions decreased, and the BSFC increased. Gorbatenko et al. (2019) studied the impact of the addition of n-butanol on the ignition delay of premixed engines in a rapid compression machine. The n-butanol addition increased the ignition delay time at low temperatures, while the branched-chain reaction of hydrogen atom abstraction due to the hydroxyl group of the γ-site and hydroperoxyl group of the α-site of the n-butanol became more dominant at high temperatures. The resultant free radicals promoted ignition. Rosdia et al. (2019) conducted experiments on the power, fuel economy, and emissions of fuel oil blends, gasoline blends, and pure gasoline in a 1.8-L turbocharged four-cylinder gasoline engine. The results of this study demonstrated that fuel oil blends increase the mean effective pressure of the internal combustion engine and BSFC. Nguyen et al. (2019) performed an experimental study on fuel reforming coupled with EGR in a direct-injection gasoline engine. Although the indicated efficiency of the internal combustion engine improved by fuel reforming, the effective efficiency of the crankshaft output increased insignificantly. This is because the increase in the concentration of hydrogen in the reactants after the fuel reforming increased the heat loss. At the same time, as the EGR opening increased, the actual intake pressure decreased, which is equivalent to an increase in the friction loss. Feng et al. (2018) and Liu et al. (2019) independently studied the combustion process of n-butanol and methanol. Liu et al. (2019) analyzed the mechanism of soot formation for methanol–gasoline blends in a co-flow diffusion flame and observed that M80 produced nearly no soot, while methanol had a significant inhibitory effect on soot precursors. Feng et al. (2018) studied the engine power and fuel

economy in the n-butanol–gasoline dual-fuel mode and showed that blending alcohol fuels could increase the maximum in-cylinder pressure, thereby improving the thermal efficiency. Gong et al. (2018) analyzed the effect of spark timing on formaldehyde and unburned methanol emissions by combining gas chromatography and liquid chromatography (GCLC) as well as gas chromatography and the light spectrum (GCLS) to collect formaldehyde emissions from a methanol–gasoline internal combustion engine using bag and absorbent sampling. The results of this study demonstrated that retarding the spark timing increased the formaldehyde emissions but decreased the emissions of unburned methanol. Hao et al. (2019) measured and analyzed the composition of $PM_{2.5}$ emissions of light-duty diesel vehicles (LDDV), heavy-duty diesel vehicles (HDDV), natural gas vehicles (NGV), light-duty gasoline vehicles (LDGV), and methanol vehicles (MV). The mass fractions of elemental carbon, organic carbon, and water-soluble ions in the components of $PM_{2.5}$ were the highest. Among the emission results of the five vehicle types, the total emissions of elemental and organic carbon from MV were the lowest. Bicer and Dincer (2018) conducted life cycle assessments on ten types of present-day vehicles including hydrogen, compressed natural gas, diesel, gasoline, liquefied petroleum gas, methanol, ammonia, hybrid electric, renewable mix, and electric vehicles. Figure 1 shows the life cycle assessments of the vehicles in terms of the human toxicity and ozone layer.

The results in Fig. 1 provide evidence that electric and plug-in hybrid electric vehicles yield a higher human toxicity than MV during the manufacturing and maintenance phases. The value of the human toxicity for electric vehicles reached 0.25 kg 1,4-DB eq km^{-1}, whereas the value for vehicles powered by methanol was less than 0.05 kg 1,4-DB eq km^{-1}. Hence, MV are less harmful to the environment than traditional gasoline and diesel vehicles. According to previous studies, methanol–gasoline blends with methanol volume fractions above 25% tend to phase-separate. Thus, the volume fractions of methanol used in this study were 15% and 100%. Experiments on the engine power, fuel economy, and unregulated emissions were performed in a naturally aspirated four-cylinder spark-ignition engine. In this study, we also measured the physicochemical properties of methanol based on the test conditions listed in Table 1. Leach et al. (2018) studied the effect of E85 on the particulate number (PN) concentration by varying the EGR, exhaust backpressure, and excess air ratio in a small highly boosted gasoline engine. The results showed that E85 has lower PN emissions across the operating range. However, the gasoline–ethanol–methanol (GEM) blended fuel exhibits entirely different particulate matter (PM) concentrations depending on the operating conditions. Furthermore, due to the lower heating value of methanol than gasoline, a higher compression ratio (CR) may be a solution. The CR directly affects the indicated efficiency of the engine. At a constant mechanical efficiency, increasing the indicated efficiency can improve the effective efficiency of an internal combustion engine. In this study, we analyze the effects of different CRs on the unregulated emissions of methanol by a small single-cylinder gasoline engine.

Experimental Configuration

Methanol (CH_3OH) is a next-generation biofuel, which belongs to the alcohol family and consists of one carbon atom (single bond). Table 1 lists the physicochemical properties of methanol. Previous studies

have reported that methanol–gasoline blends with methanol volume fractions exceeding 25% tend to phase-separate.

Accordingly, the power and fuel economy of methanol–gasoline blends with methanol volume fractions of 15% and 100% as well as pure gasoline were compared in this study.

The formaldehyde emissions of methanol–gasoline blends with methanol volume fractions of 0%, 15%, and 100% were measured under different engine loads. Table 2 lists the parameters of the experimental engine. The combustion process of an internal combustion engine is a complex multi-physics coupled field of temperature, pressure, and turbulence intensity. The direct solution is complex and costly; thus analyses of the reaction path of unregulated emissions are challenging. Therefore, this discipline has also attracted significant attention (Luong et al., 2017; Wu et al., 2018; Wei et al., 2019).

Table 2
Parameters of the internal combustion engine.

Item	Value
Model	4G15S
Displacement (mL)	1488
Power (kW)/Speed (r/min)	78/6,000
Torque (Nm)/Speed (r/min)	134/4,500
Valves	16
Bore × Stroke (mm)	76 × 82
IVO (0.5—mm lift)	10°ATDC
IVC (0.5—mm lift)	51°ABDC
EVO (0.5—mm lift)	46°BBDC
EVC (0.5—mm lift)	16°BTDC
[a]IVO, inlet valve open, °; IVC, inlet valve closed, °; EVO, exhaust valve open,	
°; EVC, exhaust valve closed, °	

Extensive simulation studies on the combustion process of internal combustion engines have been conducted. Typical simulation methods include large-eddy simulations on one-eighth of a combustion chamber. More precise simulation models yield more reliable results as well as a higher stiffness with respect to the equations (Wu et al., 2018); Consequently, the calculation cost also increases. Thus, in this study, the CR was varied to adjust the maximum combustion pressure to compare the change in unregulated emissions at different CRs. Table 3 lists the parameters of the adjustable single-cylinder gasoline engine used in the experiment. In the experiment, the maximum CR of M15 (15% volume fraction

of methanol and 85% volume fraction of gasoline) was set to 7.8, while the maximum CR of M100 (pure methanol) was set to 10.0 to mitigate the damage to the internal combustion engine from the knock of the methanol–gasoline blends. The speed was controlled at 900 rpm, the intake air temperature was 307 ± 0.5 K, and the ignition advance angle, which significantly affects the combustion and emissions according to earlier work (Wei et al., 2019), was fixed at 13° BTDC. The CR was adjusted to a smaller value such that the knock meter readings of different ratios of methanol–gasoline blends were identical.

Table 3
Parameters of the single-cylinder engine.

Parameter	Value
Cylinder diameter (mm)	65 mm
Stroke (mm)	100
Power (kW)/Speed (r/min)	2.1/1300
Working volume of cylinder (L)	0.332
Adjustment range of compression ratio	4–12
Oil pressure (kPa)	172–207
Cooling method	Water-cooled

Results And Analysis

In this study, both the external and load characteristics of a spark-ignition engine fueled with different volume fractions of methanol were measured. A comparative analysis was performed on the methanol–gasoline blends of different volume fractions (M0, M15, and M100) to evaluate the power and fuel economy of the engine when using methanol–gasoline blends. Co-solvents were not added to the methanol–gasoline blends during the experiments and the throttle of the methanol–gasoline engine was kept open. The water and oil temperatures were also kept constant. An AVL 444 gas analyzer was used to measure the excess air ratio of the engine exhaust. When the excess air ratio was equal to 1, the relationships between the three performance indicators of the engine, that is, the effective power (Pe), torque (Me), fuel consumption rate (be), and engine speed (n), were measured. The fuel consumption rate was also calculated to obtain the fuel consumption ratios of M0, M15, and M100, that is, the methanol–gasoline blends with methanol volume fractions of 0%, 15%, and 100%, respectively. In addition, the changes in the formaldehyde emissions with the methanol ratio under different engine loads were measured. Figure 2 shows the engine performance at 100% load for different methanol ratios.

The external characteristic curve of gasoline in Fig. 3 indicates that the torque reached a maximum value at a particular speed. Below this speed, the in-cylinder flow weakened, the flame velocity decreased, and the leakage and heat loss increased. Above this speed, the friction loss, accessory consumption, and pumping loss substantially increased with the increase in the speed. As a result, the torque did not

increase because of the increasing mechanical losses. As shown in Fig. 2, the power curve of gasoline is proportional to the torque multiplied by the speed. Thus, the gasoline power curve first increases with the speed.

After reaching a particular speed, the rate of the decrease in the torque is higher than the rate of the increase in the speed, which causes the power to decrease. In Fig. 2, the torque of M15 is lower than that of gasoline. When the speed was varied, the torque of M100 was higher than that of M15 and gasoline. This is because methanol's latent heat associated with vaporization is higher than that of gasoline. Based on Eq. (1) (Frenklach et al., 2019), the heat loss at the wall surface is the smallest for M100:

$$\frac{\partial Q_\omega}{\partial \theta} = h_C \times A \times (T_g - T_\omega) \quad (1)$$

where T_g is the exhaust gas temperature (K) and h_C is the heat transfer coefficient ($W/m^2 \cdot K$) (Natesan et al., 2019).

The power, in descending order, is M100 > gasoline > M15, which indicates that, as the speed increases, the torque reduction rate of M100 is the smallest, whereas those of gasoline and M15 are comparable.

The latent heat of vaporization of M100 is higher than that of gasoline. As a result, the exhaust temperature is low, where A represents the heat transfer area, with a minimal wall surface heat loss. The power curves of M100 and M15 are comparable to that of gasoline. At low speeds, the friction losses near the piston and tappet are the largest, resulting in a low mechanical efficiency associated with M100. Figures 3, 4, and 5 show the load characteristics and changes in the formaldehyde emissions due the loading of gasoline, M15, and M100, respectively.

According to Table 1, the LHV of methanol is significantly lower than that of gasoline. As a result, the BSFC increases with the increase in the volume fraction of methanol and M100 has the highest BSFC. In addition, the combustion product of methanol is formaldehyde. With an increase in the volume fraction of methanol, the total formaldehyde emissions linearly increase at each power. The results in Figs. 2, 4, and 5 demonstrate that the power of M100 corresponding to the lowest formaldehyde emissions is ~ 19.2 kW.

Compared with M15 and gasoline, the power of the methanol–gasoline blends corresponding to the lowest formaldehyde emissions in descending order is $P_{EM100} > P_{EM15} > P_{Egasoline}$. The selection of a higher power operating condition at 2,000 rpm for the spark-ignition engine fueled with M100 reduces the formaldehyde emissions without affecting the power and fuel economy of the internal combustion engine.

In the experiment, the maximum CR of M15 (15% volume fraction of methanol and 85% volume fraction of gasoline) was set to 7.8, while the maximum CR of M100 (pure methanol) was set to 10.0 to mitigate

the damage to the cylinder liner and bearing bush as a result of the knocking of the methanol–gasoline blends. The test speed was controlled at 900 rpm, with an intake air temperature of 307 ± 0.5 K. Figure 6 demonstrates that the PM mass concentration positively correlates with the CR.

The Otto cycle resulting from heating an ideal gas reduces the heat dissipation of the ideal Otto cycle as the CR increases, thereby improving the indicated thermal efficiency. However, an increase in the CR increases the in-cylinder turbulence intensity and the combustion rate further accelerates. The PM mass concentration decreases as the methanol concentration increases. This can be explained by the oxygen content of methanol, which leads to more oxygenated PM. A non-uniform premixed gas forms locally, which increases the mass concentration emission. Figure 6 also shows that the increased methanol ratio reduces the PM concentration of M100 below that of M15. This result is consistent with the observations of Li et al. (2009) and Uslu and Celik (2020) based on the process of soot surface growth who reported that the addition of lower alcohols dilutes the concentration of soot precursors, thereby inhibiting soot emissions.

Conclusions

The external and load characteristics of a spark-ignition engine fueled with different volume fractions of methanol were determined in this study. In addition, unregulated emission tests and PM emission tests with varying CRs were performed on methanol–gasoline blends with different volume fractions (M0, M15, and M100). Based on the experiments, the following conclusions can be drawn:

As the speed increases, the torque reduction rate of M100 becomes the smallest, whereas the torque reduction rates of gasoline and M15 are comparable. The power in descending order is M100 > gasoline > M15. Thus, methanol reduces the heat loss at the wall surface. The power of the methanol–gasoline blends corresponding to the lowest formaldehyde emissions in descending order is $P_{EM100} > P_{EM15} > P_{Egasoline}$. The selection of higher power operation at 2,000 rpm for the spark-ignition engine fueled with M100 reduces the formaldehyde emissions without affecting the power and fuel economy of the internal combustion engine.

As the ratio of methanol in gasoline increases, the PM emissions decrease. On the other hand, the PM emissions are positively correlated with the CR. The addition of lower alcohols dilutes the concentrations of soot precursors, thereby reducing the soot emissions.

Declarations

Ethics approval and consent to participate

Not applicable

Consent for publication

Not applicable

Availability of data and materials

The datasets used and/or analyzed during the current study are available from the corresponding author on reasonable request.

Competing interests

The authors declare that they have no competing interests.

Funding

The study was financially supported by the National Science Foundation of China [grant number: 51806020] and the Special Fund for Basic Scientific Research of Central Colleges, Chang'an University [grant number: 300102229104]. The funding sources had no role in the study design; in the collection, analysis and interpretation of data; in the writing of the report; or in the decision to submit the article for publication.

Authors' contributions

The experiments were designed and conducted by Jibai Wang Zheng Jing. Jibai Wang wrote the original draft of the manuscript. The guidance for conducting the research and preparing the manuscript were provided by Prof. Peng Zhang and Prof. Chunhua Zhang, Jibai Wnag's supervisors.

Acknowledgements

Not applicable.

References

1. Awad OI, Mamat R, Ali OM, Sidik, NAC, Yusaf, T, Kadirgama, K, Kettner, M (2018) Alcohol and ether as alternative fuels in spark-ignition engine: A review. Renew. Sustain. Energy Rev. 82:2586-2605.
2. Benajes, J, García, A, Monsalve-Serrano, J, Boronat, V (2017) Gaseous emissions and particle size distribution of dual-mode dual-fuel diesel-gasoline concept from low to full load. Appl. Therm. Eng. 120:138-149.
3. Bharathiraja, M, Venkatachalam, R, Senthilmurugan, V (2019) Performance, emission, energy and exergy analyses of gasoline fumigated DI diesel engine. J. Therm. Anal. Calorim. 136:281-293.

4. Bicer, Y, Dincer, I (2018) Life cycle environmental impact assessments and comparisons of alternative fuels for clean vehicles. Resour. Conserv. Recycl. 132:141-157.
5. Carvalho L, Lundgren, J, Wetterlund, E, Wolf, J, Furusjő, E (2018) Methanol production via black liquor co-gasification with expanded raw material base–Techno-economic assessment. Appl. Energy 225:570-584.
6. Chen, W, Zong, R, Zhao, J, Zhou, X, Li, C (2019) Clean conversion of methanol to high octane components on ZnI2 catalyst. Energy Sources, Part A, doi:10.1080/15567036.2019.1604892.
7. Cheng, CH, Cheung, CS, Chan, TL, Lee, SC, Yao, CD, Tang, KS (2008) Comparison of emissions of a direct injection diesel engine operating on biodiesel with emulsified and fumigated methanol. Fuel 87: 1870-1879.
8. Dabas, N, Dubey, V, Chhabra, M, Dwivedi, G (2019) Performance analysis of an ic engine using methanol, ethanol, and its blend with gasoline and diesel as a fuel, Adv. Fluid Thermal Eng. In: Saha P, Subbarao P, Sikarwar B (eds) Advances in fluid and thermal engineering. Lecture Notes in Mechanical Engineering. Springer, Singapore.
9. Feng, D, Wei, H, Pan, M, Zhou, L, Hua, J (2018) Combustion performance of dual-injection using n-butanol. Energy 160:573-581.
10. Frenklach, M (2002) Reaction mechanism of soot formation in flames. Phys. Chem. Chem. Phys. 4: 2028-2037.
11. Frenklach, M, Singh, RI, Mebel, AM (2019) On the low-temperature limit of HACA. Proc. Combust. Inst. 37:969-976.
12. Gong, C, Huang, W, Liu, J, Wei, F, Yu, J, Si, X, Liu, F, Li, Y (2018) Detection and analysis of formaldehyde and unburned methanol emissions from a direct-injection spark- ignition methanol engine. Fuel 221:188-195.
13. Gorbatenko, I, Tomlin, AS, Lawes, M, Cracknell, RF (2019) Experimental and modelling study of the impacts of n-butanol blending on the auto-ignition behaviour of gasoline and its surrogate at low temperatures. Proc. Combust. Inst. 37:501-509.
14. Hagos, FY, Ali, OM, Mamat, R, Abdullah, AA (2017) Effect of emulsification and blending on the oxygenation and substitution of diesel fuel for compression ignition engine. Renew. and Sustain. Energy Rev. 75:1281-1294.
15. Hao YZ, Gao, C, Deng, S, Yuan, M, Song, W, Lu, Z, Qiu, Z (2019) Chemical characterization of PM2.5 emitted from motor vehicles powered by diesel, gasoline, natural gas and methanol fuel. Sci. Total Environ. 674:128-139.
16. Huang, HZ, Zhou, CZ, Liu, QS, Wang, QX, Wang, XQ (2016) An experimental study on the combustion and emission characteristics of a diesel engine under low temperature combustion of diesel/gasoline/n-butanol blends. Appl. Energy 170:219-231.
17. Huang, HZ, Zhu, JZ, Zhu, ZJ, Wei, HL, Lv, DL, Zhang, P, Sun, H (2017) Development and validation of a new reduced diesel-butanol blends mechanism for engine applications. Energy Convers. Manage. 149:553-563.

18. Huang, H, Zhu, H, Zhang, Q, Li, C (2018) Effect of acidic properties of hierarchical HZSM-5 on the product distribution in methanol conversion to gasoline. Korean J. Chem. Eng. 35(3):1-9.
19. Jin, C, Yao, M, Liu, H, Lee, C-FF, Ji, J (2011) Progress in the production and application of n-butanol as a biofuel. Renew. Sustain. Energy Rev. 15:4080-4106.
20. Kumar, BR, Saravanan, S (2016) Effects of iso-butanol/diesel and n-pentanol/diesel blends on performance and emissions of a DI diesel engine under premixed LTC (low temperature combustion) mode. Fuel 170:49-59.
21. Leach, FCP, Stone, R, Richardson, D, Turner, JWG, Lewis, A, Akehurst, S, Remmert, S, Campbell, S, Cracknell, R (2018) The effect of oxygenate fuels on PN emissions from a highly boosted GDI engine. Fuel 225:277-286.
22. Li YY, Zhang L, Tian Z, Yuan T, Wang J, Yang B, Qi F (2009) Experimental study of a fuel-rich premixed toluene flame at low pressure. Energy Fuels 23:1473-1485. https://doi.org/10.1021/ef800902t
23. Liu, F, Hua, Y, Wu, H, Lee, C-F, Shi, Z (2019) Experimental and kinetic studies of soot formation in methanol-gasoline coflow diffusion flames. J. Energy Inst. 1: 38-50.
24. Liu, H, Wang, Z, Zhang, J, Wang, J, Shuai, S (2017) Study on combustion and emission characteristics of Polyoxymethylene Dimethyl Ethers/diesel blends in light-duty and heavy-duty diesel engines. Appl. Energy 185:1393-1402.
25. Luong, MB, Yu, GH, Chung, SH, Yoo, CS (2017) Ignition of a lean PRF/air mixture under RCCI/SCCI conditions: Chemical aspects. Proc. Combust. Inst. 36:3587-3596. https://doi.org.10.1016/j.proci.2016.06.076
26. Natesan, V, Periyasamy, S, Muniappan, K, Rajamohan, S (2019) Experimental investigation and exergy analysis on homogeneous charge compression ignition engine fueled with natural gas and diethyl ether. Environ. Sci. Pollut. Res. 26:6677-6695.
27. Nguyen, D-K, Sileghem, L, Verhelst, S (2019) Exploring the potential of reformed-exhaust gas recirculation (R-EGR) for increased efficiency of methanol fueled SI Engines. Fuel 236:778-791.
28. Reitz, RD, Duraisamy, G (2015) Review of high efficiency and clean reactivity controlled compression ignition (RCCI) combustion in internal combustion engines. Prog. Energy Combust. Sci. 46:12-71.
29. Rosdia, SM, Mamata, R, Azri, A, Sudkahar, K, Yusri, IM (2019) Evaluation of properties on performance and emission to turbocharged SI engine using fusel oil blend with gasoline. IOP Conf. Ser. Mater. Sci. Eng. 494:01201.
30. Samimi, F, Feilizadeh, M, Ranjbaran, M, Arjmand, M, Rahimpour, MR (2018) Phase stability analysis on green methanol synthesis process from CO_2 hydrogenation in water cooled, gas cooled and double cooled tubular reactors. Fuel Process. Technol. 181:375-387.
31. Schifter, I, Diaz, L, Gonzalez, U, Gonzalez-Macias, C, Mejía-Centeno, I (2019) The effects of addition of co-solvents on the physicochemical properties of gasoline-methanol blended fuels. Int. J. Engine Res. 20:501-509.

32. Sharifi, K, Halladj, R, Royaee, SJ, Nasr, MRJ (2019) Investigation of the effect of HZSM-5 over HDS and reforming processes for clean gasoline production. Int. J. Environ. Sci. Technol. 16:865-874.
33. Shirazi, SA, Abdollahipoor, B, Martinson, J, Windom, B, Foust, TD, Reardon, KF (2019) Effects of dual-alcohol gasoline blends on physiochemical properties and volatility behavior. Fuel 252:542-552.
34. Tartakovsky, L, Sheintuch, M (2018) Fuel reforming in internal combustion engines. Prog. Energy Combust. Sci. 67:88-114.
35. Tian, XL, Zhong, MH, Shi, CL, Zhang, PH, Liu, C (2018) Experimental study of the combustion characteristics of methanol--gasoline blends pool fires in a full-scale tunnel. Fire Mater. 42:386-393.
36. Tucki, K, Mruk, R, Orynycz, O, Wasiak, A, Botwińska, K, Gola, A (2019) Simulation of the operation of a spark ignition engine fueled with various biofuels and its contribution to technology management. Sustainability 11:27-99.
37. Uslu, S, Celik, MB (2020) Combustion and emission characteristics of isoamyl alcohol- gasoline blends in spark ignition engine. Fuel 262:116496. https://doi.org/10.1016/j.fuel.2019.116496
38. Wang, CM, Li, YF, Xu, CS, Badawy, T, Sahu, A, Jiang, CZ (2019) Methanol as an octane booster for gasoline fuels. Fuel 248:76-84.
39. Wang, YS, Jiang, XY, Wu, ZX (2015) Study on control and performances of diesel- methanol compound combustion vehicle, 2015 8th International Conference on Intelligent Networks and Intelligent Systems (ICINIS), Tianjin, People's Republic of China, Nov 1–3, 2015.
40. Wu, ZK, Rutland, CJ, Han, Z (2018) Numerical evaluation of the effect of methane number on natural gas and diesel dual-fuel combustion. Int. J. Engine Res. 20:1-19. https://doi.org/10.1177/1468087418758114
41. Wei, SL, He, CH, Liu, X, Song, ZL (2019) Numerical analysis of the effects of swirl ratio on the performance of diesel engine fueled with n-butanol–diesel blends. J. Energy Eng. 145(3):04019005.
42. Wei, HQ, Zhao, WH, Qi, JY, Liu, ZK, Zhou, L (2019) Effect of injection timing on the ignition process of n-heptane spray flame in a methane/air environment. Fuel 245:345-359.
43. Yao, CD, Cheung, CS, Cheng, CH, Wang, YS, Chan, TL, Lee, SC (2008) Effect of diesel/methanol compound combustion on diesel engine combustion and emissions. Energy Convers. Manage. 49:1696-1704.
44. Yarulina, I, Chowdhury, AD, Meirer, F, Weckhuysen, BM, Gascon, J (2018) Recent trends and fundamental insights in the methanol-to-hydrocarbons process. Nat. Catal. 1:398-411.
45. Yue, ZY, Reitz, RD (2019) Numerical investigation of radiative heat transfer in internal combustion engines. Appl. Energy 235:147-163.

Figures

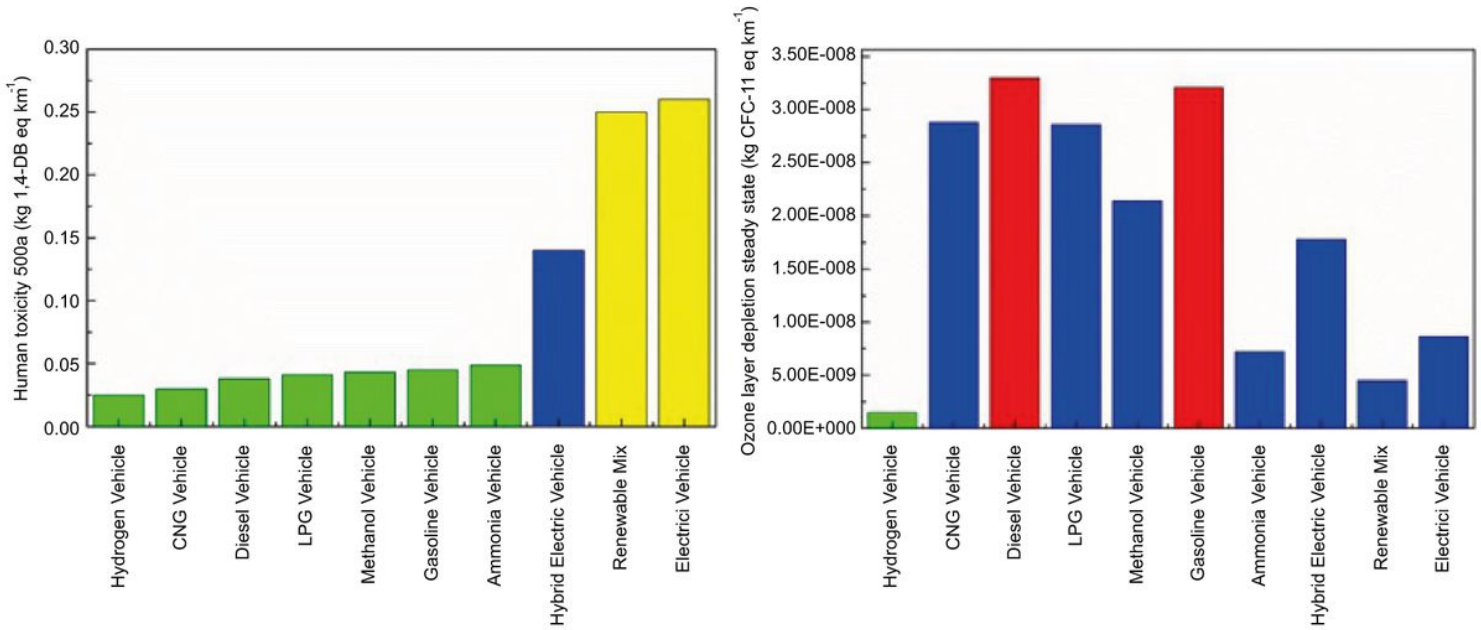

Figure 1

Life cycle assessment of the (a) human toxicity and (b) ozone layer depletion.

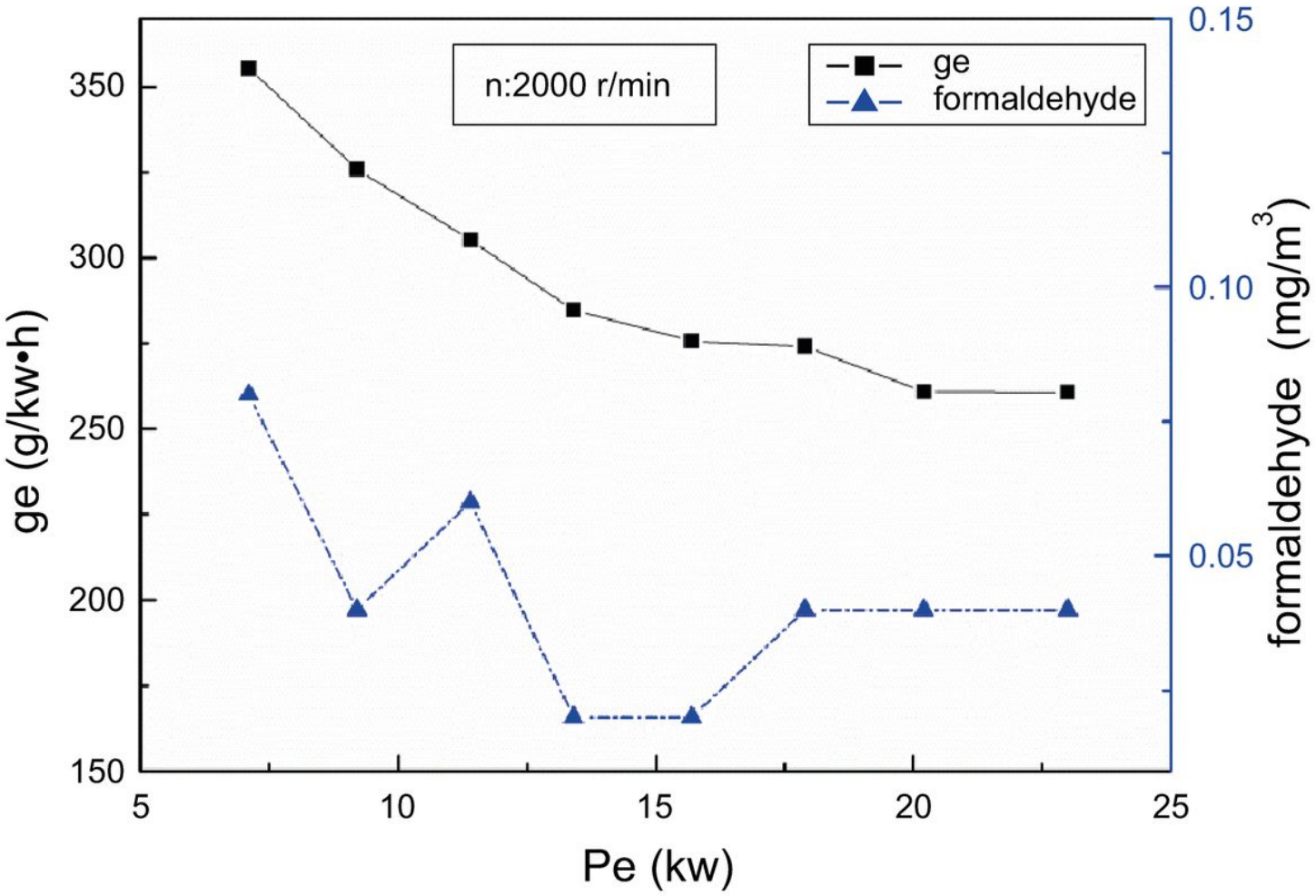

Figure 2

Engine performance of methanol–gasoline blends at 100% full load.

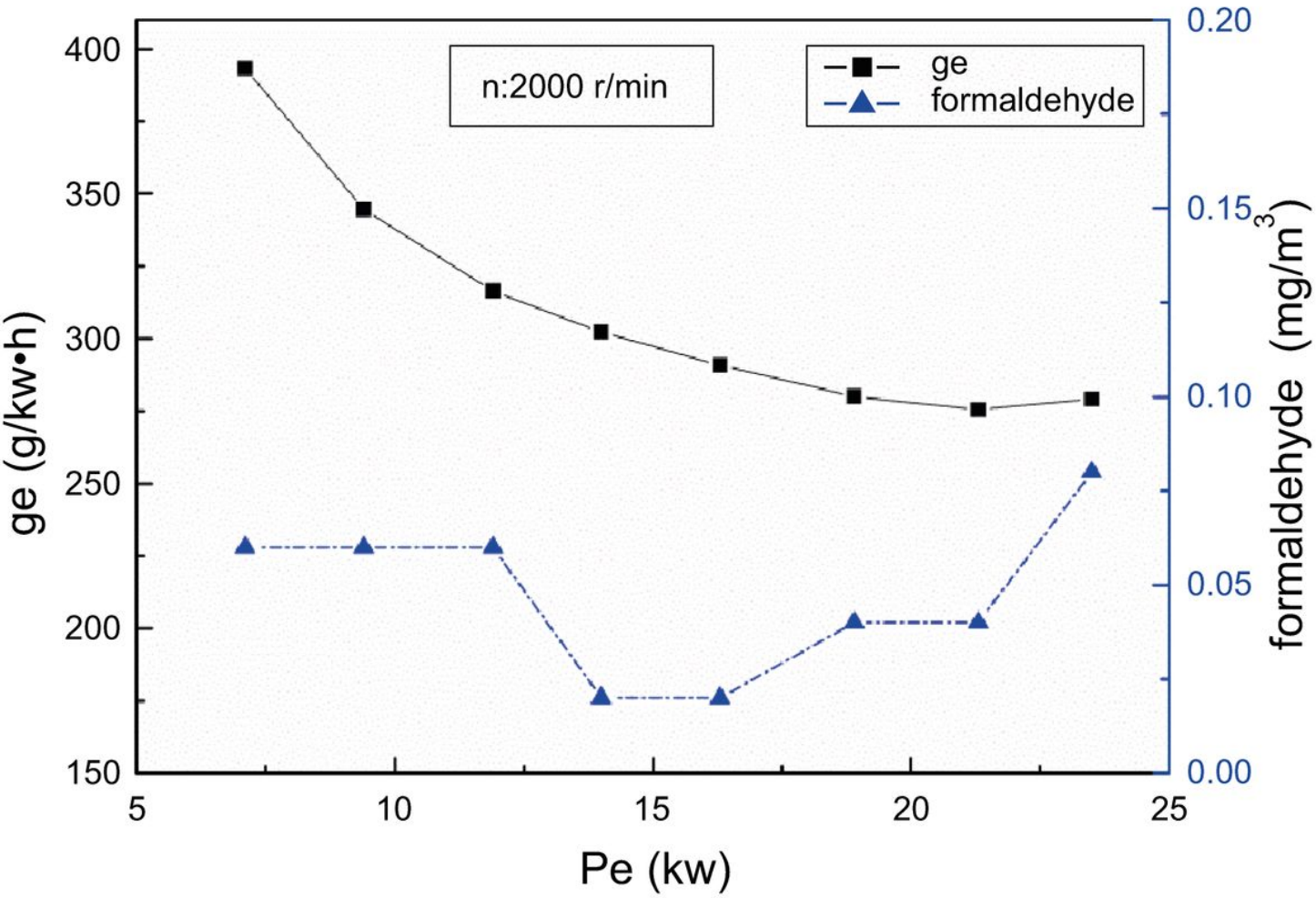

Figure 3

Formaldehyde emissions of gasoline under different engine loads.

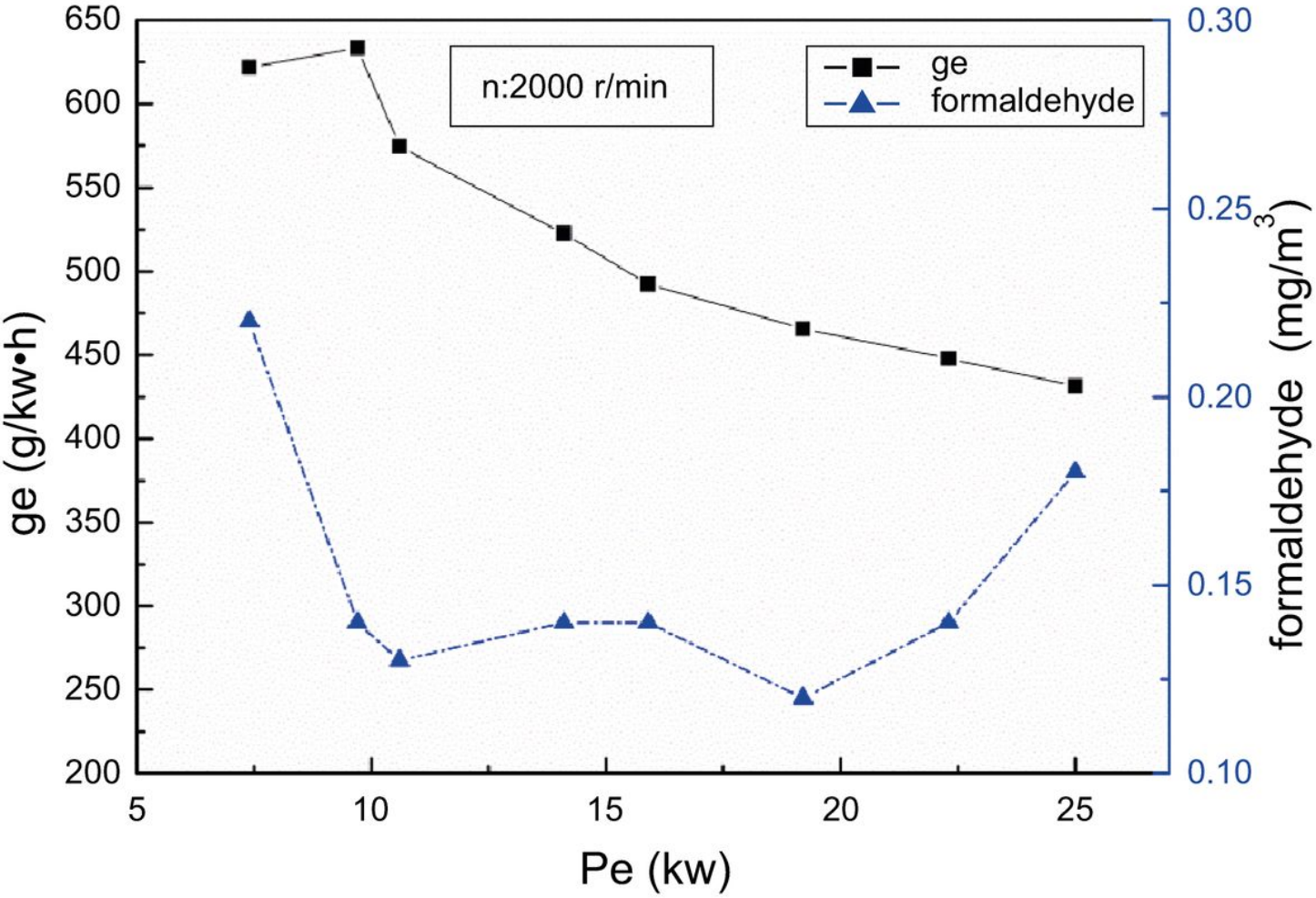

Figure 4

Formaldehyde emissions of M15 under different engine loads.

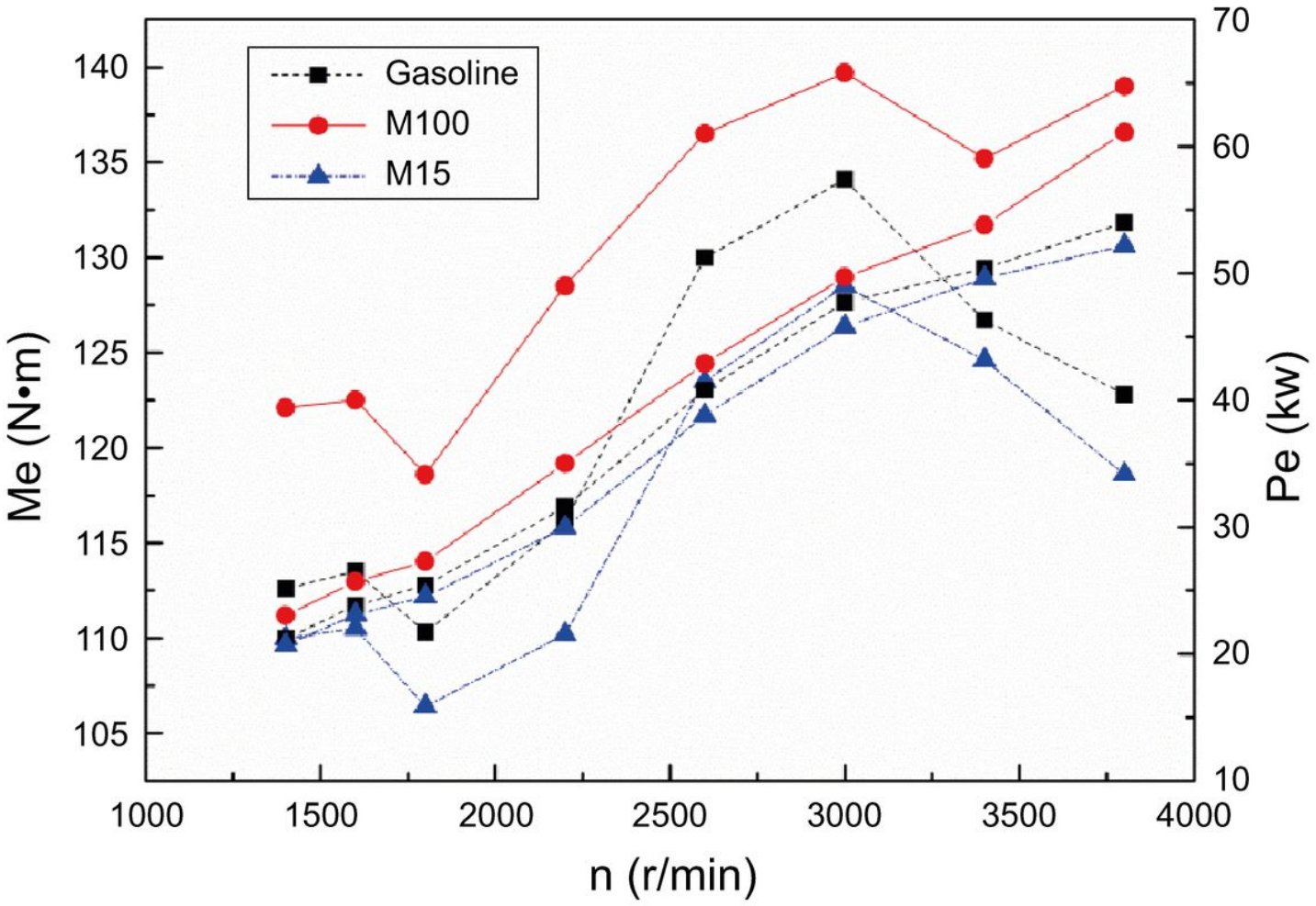

Figure 5

Formaldehyde emissions of M100 under different engine loads.

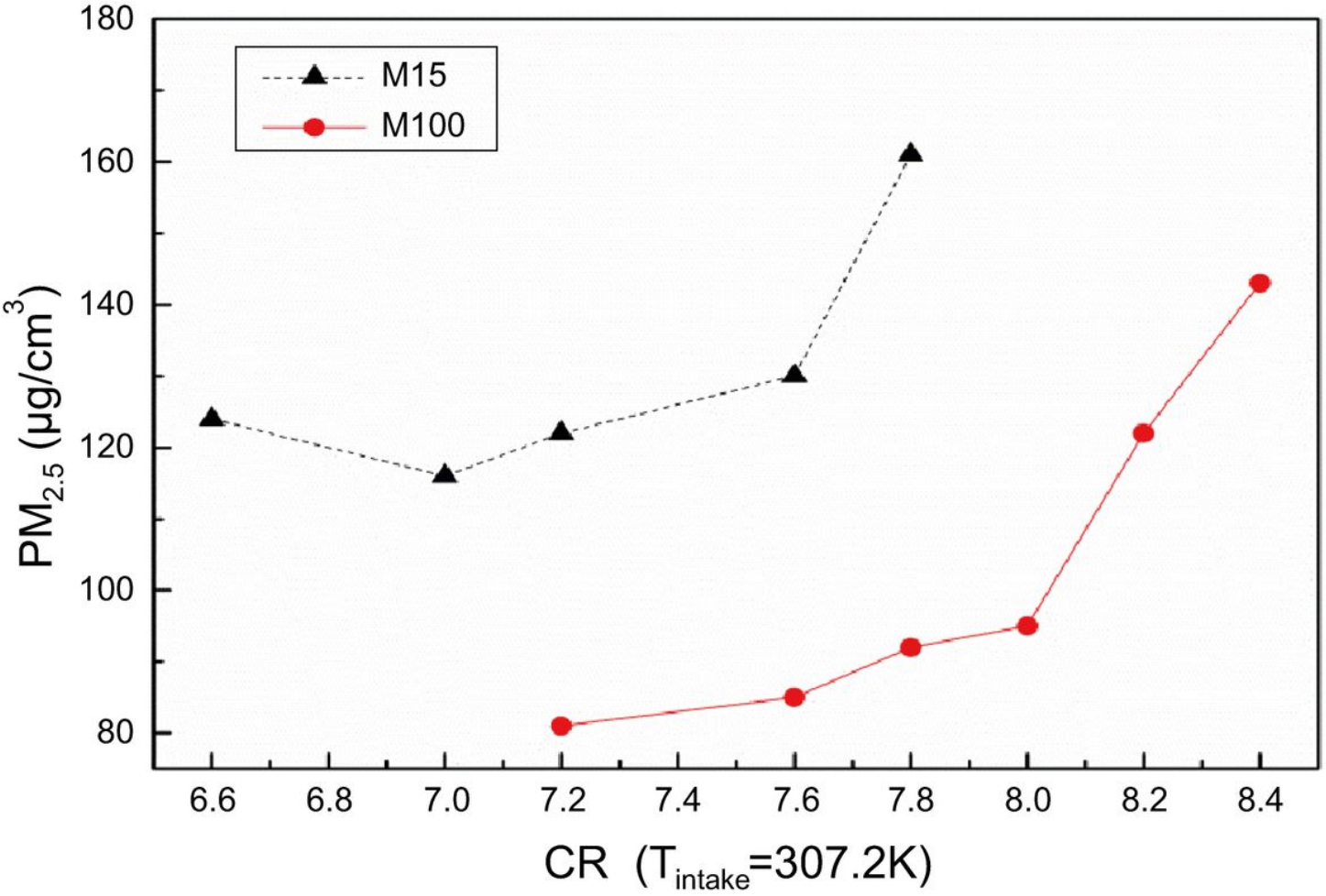

Figure 6

Effects of the compression ratio (CR) on the PM2.5 emissions.